

1 REVISION 1

3 Dolomite-IV: candidate structure for a carbonate in the 4 Earth's lower mantle

5
6 Marco Merlini¹, Valerio Cerantola², G. Diego Gatta¹, Mauro Gemmi³, Michael Hanfland², Ilya Kupenko^{2,4},
7 Paolo Lotti¹, Harald Müller², Li Zhang⁵

8
9 ¹Università degli Studi di Milano, Dipartimento di Scienze della Terra, Via Botticelli, 23 20133 Milano (Italy)

10 ²ESRF, The European Synchrotron 71, Avenue des Martyrs, 38043 Grenoble (France)

11 ³Center for Nanotechnology Innovation@NEST, Istituto Italiano di Tecnologia, Piazza San Silvestro, 12,
12 56127, PISA, Italy

13 ⁴Institute for Mineralogy, Westfälische Wilhelms-Universität, Corrensstraße 24, 48149 Münster, Germany

14 ⁵Center for High Pressure Science and Technology Advanced Research (HPSTAR), Shanghai 201203 (China)

16 **Abstract**

17 We report the crystal structure of dolomite-IV, a high-pressure polymorph of Fe-dolomite stabilized at 115
18 GPa and 2500 K. It is orthorhombic, Space Group *Pnma*, $a=10.091(3)$ $b=8.090(7)$ $c=4.533(3)$ Å $V=370.1(4)$ Å³
19 at 115.2 GPa and ambient temperature. The structure is based on the presence of 3-fold C₃O₉ carbonate
20 rings, with carbon in tetrahedral coordination. The starting Fe-dolomite single crystal during compression
21 up to 115 GPa transforms into dolomite-II (at 17 GPa) and dolomite-IIIb (at 36 GPa). The dolomite-IIIb,
22 observed in this study, is rhombohedral, Space Group *R3*, $a=11.956(3)$ $c=13.626(5)$ Å, $V=1686.9(5)$ Å³ at
23 39.4 GPa. It is different from a previously determined dolomite-III structure, but topologically similar. The
24 density increase from dolomite-IIIb and dolomite IV is ca. 3%. The structure of dolomite-IV has not been
25 predicted, but it presents similarities with the structural models proposed for the high-pressure
26 polymorphs of magnesite, MgCO₃. A ring-carbonate structure match with spectroscopic analysis of high
27 pressure forms of magnesite-siderite reported in the literature, and, therefore, is a likely candidate
28 structure for a carbonate at the bottom of the Earth's mantle, at least for magnesian and dolomitic
29 compositions.

31 **Introduction**

32

33 Minor and trace elements in the Earth's mantle play an important role in geochemical processes. In recent
34 years, there has been a particular interest in the understanding of the behavior of carbon in the inner
35 Earth. It is estimated that 90 % of bulk-Earth carbon is hidden in deep reservoirs (Hazen and Schiffrics
36 2013). A significant fraction is very likely in the core, stored in intermetallic phases, such as Fe₃C or Fe₇C₃, as
37 suggested by the composition of iron meteorites (Anders 1964) and as recently found within super-deep
38 diamonds (Smith et al. 2016). In the upper and lower mantle, carbon may be present as elemental carbon
39 (diamond), dissolved in fluids (e.g., CH₄, CO₂), or as carbonate minerals. The occurrence of carbonate as
40 inclusions in diamonds (Berg 1986; Howell et al. 2012) indicates that the coexistence of reduced and
41 oxidized carbon form is possible. Carbonates undergo polymorphic phase transitions; therefore, the search
42 for the possible structures adopted by carbonates at high pressures and temperatures, still unclear (Hazen
43 et al. 2012), is an important issue to be addressed. Computational and experimental work suggest a rich
44 polymorphism of carbonates and their transformation at extreme conditions into complex structures
45 featuring tetrahedrally coordinated carbon (Arapan et al. 2007; Oganov et al. 2008 2013; Boulard 2011).
46 However, a full *ab initio* experimental determination of the structure of a carbonate with tetrahedrally
47 coordinated carbon and ABO₃ stoichiometry has still not been achieved. We have previously applied
48 synchrotron single-crystal diffraction on a multigrain sample after red-ox reaction of a natural Mg-siderite
49 (Merlini et al. 2015), and successfully determined the crystal structure of a new carbonate, Mg₂Fe₂(C₄O₁₃),
50 whose stoichiometry deviates from that of ABO₃, adopted by calcite, magnesite and dolomite. The results
51 indicate that, from a methodological point of view, it is possible to perform accurate single-crystal X-ray
52 diffraction and *ab initio* structure determination in non-ideal situations, with a conventional single-crystal
53 diffraction approach. From a crystal chemistry point of view, the Mg₂Fe₂(C₄O₁₃) structure confirms the
54 coordination increase from 3- to 4-fold for carbon and the pressure-induced polymerization of carbonate
55 units.

56 Here, we report a novel experimental work on Fe-dolomite studied above Mbar pressures and lower
57 mantle temperatures, with the main aim to determine a crystal structure of a carbonate with ABO_3
58 stoichiometry. Few attempts in stabilizing a single crystal of HP-magnesite have been not successful. In
59 previous studies (Mao et al. 2011; Merlini et al. 2012a), it was observed that dolomite compositions above
60 40 GPa can exist as single phases at mantle pressures and temperatures in contrast to the decomposition
61 into a mixture of aragonite/post-aragonite and magnesite seen in pure $CaCO_3$. We selected a sample with
62 the same composition (Merlini et al. 2012a) for the experiment, i.e. $Ca(Mg_{0.6}Fe_{0.4})(CO_3)_2$, expecting that also
63 at a higher pressure a single phase could be maintained, possibly without undergoing a red-ox reaction. The
64 presence of Fe in the sample is fundamental for the possibility of heating, by coupling an infrared laser to
65 the electronic structure of iron that is capable of absorbing the laser radiation. For comparison, the
66 compression behavior of pure dolomite was also investigated up to 100 GPa pressures.

67

68 **Materials and methods.**

69

70 Natural samples of Fe-dolomite from La Mure (Isere, France) were used in the current experiment, similar
71 to the sample used in a previous study (Merlini et al. 2012a). A pure sample of dolomite from Bazena (Italy)
72 was also used. Microprobe analysis was performed at the Earth Science Department (University of Milano,
73 Italy), and the results indicate a stoichiometry of $\text{Ca}(\text{Mg}_{0.6}\text{Fe}_{0.4})(\text{CO}_3)_2$ for Fe-dolomite, and pure dolomite
74 composition, $\text{CaMg}(\text{CO}_3)_2$, for the other sample used. High-pressure experiments were performed at the
75 ID09A high-pressure beamline at ESRF (Grenoble, France). We used the standard beamline setup with a
76 monochromatic beam of 0.4139 Å with a section of $10 \times 10 \mu\text{m}^2$ on the sample. The diamond anvil cell used
77 mounted two beveled diamonds, one with a 150 μm diameter culet and the second with 120 μm diameter
78 culet, bevel out of 350 μm with 9° angle. The gasket was made of Re, pre-indented to a thickness of 35 μm
79 and drilled by spark-erosion. The sample was a single crystal of ca. $10 \times 10 \times 5 \mu\text{m}^3$, deposited on a diamond
80 face in such a way that only a fraction of an edge was actually touching the diamond. The pressure
81 medium, Ne, therefore surrounded the crystal, acted as an insulating layer, and prevented any chemical
82 reaction between sample and diamonds. The high-pressure ramp, data reduction and analysis follow the
83 established protocols for the beamline (Merlini and Hanfland 2013). Structure solution was achieved with
84 the charge-flipping algorithm (Oszlányi and Suto 2010) and Fourier-difference analysis, using Super-Flip
85 (Palatinus and Chapuis 2007) and Jana software (Petříček et al. 2014). The unit-cell volume data were fitted
86 to a second- and a third-order Birch-Murnaghan EoS (BM-EoS; Birch 1947; Angel 2000) using the EOS-FIT5.2
87 program (Angel 2000). The BM-EoS parameters were simultaneously refined using the data weighted by
88 the uncertainties in P and V .

89

90 **Results**

91

92 *Fe-dolomite high pressure behavior: compressibility and phase transitions*

93

94 During the compression of the single crystal of Fe-dolomite, we observe at 17 GPa the second-order
95 dolomite-to-dolomite-II phase transition. The low pressure data were fitted to a second-order BM equation
96 of state and the results (Table 1 and supplementary data) are in agreement with the data previously
97 reported (Merlini et al. 2016). The dolomite-II structure was solved with a charge flipping algorithm. The
98 results confirm the model previously reported by Merlini et al. (2012a). It is a distortion of the dolomite
99 structure, associated by the rotation of carbonate groups. It presents a crystallographic group-subgroup
100 relation between dolomite and dolomite-II, similar to the calcite-calcite-II transition (Merrill and Basset
101 1975). Above 36 GPa, a first-order transition with volume discontinuity is observed. The unit-cell
102 parameters (Table 1) of the high-pressure polymorph are different from those reported for dolomite-III
103 (Merlini et al. 2012a), despite the similar composition of Fe-dolomite used in this and the previous studies
104 (Merlini et al. 2012a). We refer to this new polymorph as dolomite-IIIb. The structure solution for Fe-
105 dolomite-IIIb was readily achieved with a charge flipping algorithm. It crystallizes in rhombohedral
106 symmetry (space group $R\bar{3}$) with lattice parameters $a \sim 11.956$ and $c \sim 13.626$ Å at 39.4 GPa. Its topology is
107 similar to that of calcite, i.e. NaCl-type connection, with carbonate groups differently oriented in the unit
108 cell instead of the parallel arrangement as in calcite and dolomite. The tilting of carbonate groups causes an
109 increased coordination number for the cation sites and a noticeable density increase (Figure 1). We observe
110 high-pressure behavior similar to that of calcite, where a few different polymorphs can be detected in the
111 same pressure range (Merlini et al. 2012b 2014). This can be explained by the similar energy of several
112 carbonate polymorphs as shown by computational studies (e.g., Oganov et al. 2008) in a number of
113 predicted metastable structures. The volume data for Fe-dolomite-IIIb up to Mbar pressures, fitted with a
114 2nd-order BM EoS, result in a bulk modulus $K_0 = 91.0(9)$ GPa and an extrapolated volume at ambient
115 pressure of $104(1)$ Å³, i.e., a density of 3.146 g/cm³, which is 3.7 % higher than that of the $R\bar{3}c$ ambient-

116 pressure structure. The diffraction data for dolomite-IIIb at 115 GPa can still be indexed and fitted with the
117 same structure model.

118

119 *Dolomite high-pressure behavior: compressibility and phase transitions*

120

121 During the compression of pure dolomite, we observed the dolomite-to-dolomite-II transition between 14
122 and 18 GPa. The dolomite-II structure is the same dolomite-II structure observed for the Fe-bearing
123 dolomite. Dolomite-II is observed to be stable up to 40 GPa. Above 41 GPa, a new triclinic structure is
124 formed. It is labelled as dolomite-IIIc, and crystallizes in a triclinic unit-cell, which differs from those of
125 dolomite-III and dolomite-IIIb (Table 1 and supplementary materials). Any attempt to solve the structure in
126 the centrosymmetric *P*-1 space group failed, suggesting the possibility of a non-centrosymmetric symmetry.
127 The similarity of dolomite-IIIc volume with dolomite-III and IIIb, and, especially, the geometrical relationship
128 between the lattice of dolomite-IIIc and dolomite-II, suggests a unit-cell content of eight formula unit (i.e.,
129 $\text{CaMg}(\text{CO}_3)_2$; $Z=8$). Unfortunately, the number of observed diffractions is not sufficient to allow structure
130 solution and refinement with 350 variables. The diffraction patterns collected up to 100 GPa are indexed
131 with the same triclinic unit cell. The volume data for dolomite-III fitted to a BM EoS lead to an extrapolated
132 bulk modulus and volume per formula unit at ambient pressure of $K_0 = 92(6)$ GPa and $V_0 = 105(1) \text{ \AA}^3$, i.e.
133 with an ambient pressure density of 2.94 g/cm^3 , 3.5 % higher than that of dolomite. No other phase
134 transitions are observed within the *P*-range investigated. A comparison of the volume of dolomite-IIIc and
135 Fe-dolomite-IIIb polymorphs (supplementary data) indicates that Fe-dolomite-IIIb has a significantly lower
136 molar volume.

137

138 *Dolomite IV crystal structure*

139 The presence of iron in the natural Fe-dolomite crystal allowed laser heating. The sample was annealed at
140 2500 °C at 120 GPa for five minutes. After a thermal quench, X-ray diffraction showed that the crystal
141 transformed into a multigrain sample. Single crystal spots were visible in the diffraction images, and with
142 the aid of a reciprocal space visualizer, an orthorhombic lattice was successfully identified that was able to

143 index most of the diffraction peaks. Inspection of the inter-planar distances (d) of the non-indexed peaks
144 indicates that no other periodicities occur; however, the d values of non-indexed spots match those of the
145 indexed peaks. The multigrain sample, therefore, is likely a single phase. The unit-cell constants are
146 $a=10.091(3)$, $b=8.090(7)$, $c=4.533(3)$ Å, and $V=370.1(4)$ Å³ at 115.2 GPa and ambient temperature. The
147 structure solution and refinement was successfully performed in the orthorhombic *Pnma* space group.
148 Dolomite-IV is a ring carbonate. Its main feature is the presence of corner-sharing tetrahedral CO₄ units in
149 3-fold rings (Figure 2). The cations form distorted 8-fold and 10-fold coordination polyhedra. The
150 multiplicity of the two cation sites are different, and this suggests a disordered cation distribution among
151 the two sites. It was impossible to recover the sample after pressure release, because the diamonds broke
152 during decompression. A few pressure points have also been collected on decompression, in the pressure
153 range 70-115 GPa. The volume data were fitted to a 2nd order BM-EoS, leading to a bulk modulus $K_0 =$
154 $150(25)$ GPa and an ambient pressure volume of $92(1)$ Å³ per formula unit. The ambient pressure density
155 increases by 13% compared to that of dolomite-III. The density increase calculated at 115 GPa is 1% higher.
156 The normalized volume (per formula units) compared to the normalized volume of dolomite-IIIb indicates a
157 density increase of about 1.5 % (Figure 3). This is consistent with a transformation without compositional
158 change. The structure, in terms of unit cell and symmetry, does not match any predicted structure.
159 However, the ring-carbonate topology is similar to the predicted stable structures of MgCO₃ (Oganov et al.
160 2008; Pickard and Needs 2015).

161

162 **Discussion and implications**

163

164 The search for possible host structures of carbonates has stimulated computational and experimental work
165 in the last ten years. One major outcome is the prediction (Arapan et al. 2007; Oganov et al. 2006,2008
166 2013; Pickard et al. 2015; Boulard et al. 2015) and the experimental verification of the coordination change
167 of carbon in carbonates by crystal structure determination (e.g., Merlini et al. 2015) and spectroscopic
168 analysis (e.g., Boulard et al. 2011; Boulard et al. 2015). Tetrahedral carbonate units can polymerize, and a
169 comparison with silicates may suggest that the high-pressure crystal chemistry of carbonates could
170 reproduce the variability observed in ambient structures of silicates. However, as has been pointed out by
171 computational work (i.e., Oganov et al. 2013), the energy of C_2O_7 groups as a function of C-O-C angles
172 presents two marked minima, preventing all the flexibility observed in silicates, where the energy curve is
173 more flat. In the dolomite-IV ring-carbonate structure, we observe two C-O-C angles of $\sim 119^\circ$, close to the
174 predicted $\sim 123.6^\circ$. The third C-O-C angle, which completes the 3-fold ring, is $\sim 104^\circ$. Ring-carbonates are
175 predicted as stable phases for $MgCO_3$ composition (Oganov et al. 2008; Pickard et al. 2015). Few different
176 polymorphs have been calculated, but all of them present the topology observed experimentally, based on
177 layers of rings where apical oxygens in neighboring layers point in opposite directions. The experimental
178 data reported here add an interesting insight into the crystal chemistry of carbonates at extreme
179 conditions. For the first time, it has been stabilized in mixed composition, almost in the middle of the
180 compositional diagram $CaCO_3$ - $MgCO_3$ - $FeCO_3$. The cation crystal sites, two with different multiplicities,
181 indicate that Ca, Mg and Fe are statistically distributed. The ring-carbonate structure can accommodate the
182 strain arising from the variable size of Ca, Mg and Fe cations, and this observation is different, for example,
183 if compared to silicate Ca- and Mg-perovskite at high pressure, where the two end-members do not mix. A
184 ring-carbonate, therefore, represents a good candidate for a carbonate structure stable at lower mantle
185 conditions, in an Mg-rich environment. The dolomite-IV structure does not have any analogues among the
186 main silicates, except for walstromite mineral, $BaCa_2Si_3O_9$ (Dent Glasser and Glasser 1968), and the
187 walstromite-type high-pressure polymorph of $CaSiO_3$, which could be found only as inclusions in super-
188 deep diamonds (Joswig et al. 2003; Anzolini et al. 2016).

190 **References**

191

192 Anders, E. (1964) Origin, age, and composition of meteorites. *Space Science Reviews*, 3(5-6), 583-714

193 Angel, R.J. (2000) High-pressure, high-temperature crystal chemistry. *Reviews in Mineralogy and*

194 *Geochemistry*, 41, 35–59.

195 Anzolini, C., Angel, R.J., Merlini, M., Derzsi, M., Tokar, K., Milani, S., Krebs, M.Y., Brenker, F.E., Nestola, F.,

196 Harris, J.W. (2016) Depth of formation of CaSiO₃-walsstromite Included in super-deep diamonds.

197 *Lithos*, 265, 138-147.

198 Arapan, S., De Almeida, J.S., and Ahuia, R. (2007) Formation of sp³ hybridized bonds and stability of CaCO₃

199 at very high pressure. *Physical Review Letters*, 98, 268501.

200 Berg, G.W. (1986) Evidence for carbonate in the mantle. *Nature*, 324, 50–51.

201 Birch, F. (1947) Finite elastic strain of cubic crystal. *Physical Review* 71, 809-824.

202 Boulard, E., Gloter, A., Corgne, A., Antonangeli, D., Auzende, A.L., Perrillat, J.P., Guyot, F., and Fiquet, G.

203 (2011) New host for carbon in the deep Earth. *Proceedings of the National Academy of Sciences*,

204 108, 5184–5187.

205 Boulard, E., Pan, D., Galli, G., Liu, Z., and Mao, W.L. (2015) Tetrahedrally coordinated carbonates in Earth's

206 lower mantle. *Nature Communications*, 6, 6311.

207 Dent Glasser, L.S., and Glasser, F.P. (1968). The crystal structure of walsstromite. *American Mineralogist*, 53,

208 9-13

209 Hazen, R.M., and Schiffrin, C.M. (2013) Why Deep Carbon? *Reviews in Mineralogy and Geochemistry*, 75,

210 1-6.

211 Hazen, R.M., Hemley, R.J., and Mangum, A.J. (2012) Carbon in Earth's interior: storage, cycling and life.

212 *Transactions of the American Geophysical Union*, 93, 17–28.

213 Howell, D., Wood, I.G., Nestola, F., Nimis, P. and Nasdala, L. (2012) Inclusions under remnant pressure in

214 diamond: a multi-technique approach. *European Journal of Mineralogy*, 24, 563-573.

215 Joswig, W., Paulus, E.F., Winkler, B., and Milman, V. (2003) The crystal structure of CaSiO₃-walsstromite, a

216 special isomorph of wollastonite-II. *Zeitschrift für Kristallographie*, 218, 811–818.

217 Mao, Z., Armentrout, M., Rainey, E., Manning, C.E., Dera, P., Prakapenka, V.B., and Kavner, A. (2011)

218 Dolomite III: a new candidate lower mantle carbonate. *Geophysical Research Letters*, 38, L22303.

219 Merlini, M., and Hanfland, M. (2013) Single-crystal diffraction at megabar conditions by synchrotron

220 radiation. *High Pressure Research*, 33, 511–522.

221 Merlini, M., Crichton, W., Hanfland, M., Gemmi, M., Mueller, H., Kuppenko, I., and Dubrovinsky, L. (2012a)

222 Dolomite-II and dolomite-III: crystal structures and stability in the Earth's lower mantle.

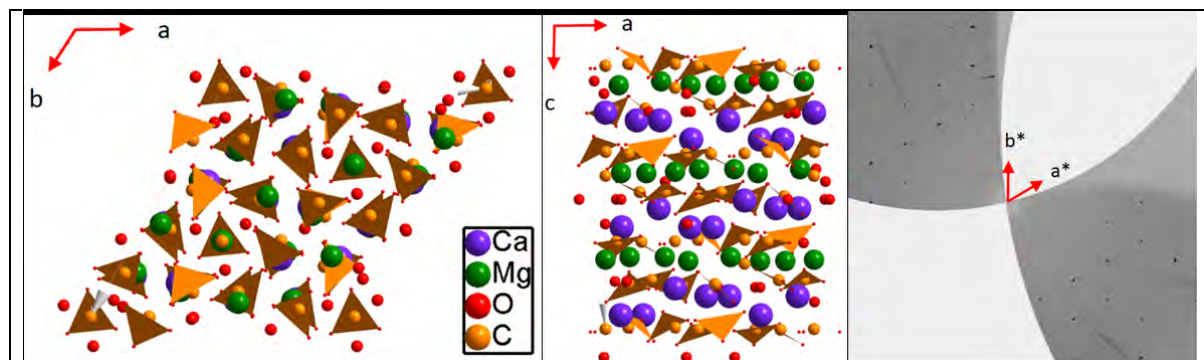
223 *Proceedings of the National Academy of Sciences of the United States of America*, 109(34), 13509-

224 13514

- 225 Merlini, M., Hanfland, M., and Crichton, W. (2012b) CaCO₃-III and CaCO₃-VI, high-pressure polymorphs of
226 calcite: possible host structures for carbon in the Earth's mantle. *Earth and Planetary Science*
227 *Letters*, 333-334, 265-271.
- 228 Merlini, M., Crichton, W.A., Chantel, J., Guignard, J., and Poli, S. (2014) Evidence of interspersed co-existing
229 CaCO₃-III and CaCO₃-IIIb structures in polycrystalline CaCO₃ at high pressure. *Mineralogical*
230 *Magazine*, 78, 225-233
- 231 Merlini, M., Hanfland, M., Salamat, A., Petitgirard, S., and Müller, H. (2015) The Crystal Structures of
232 Mg₂Fe₂C₄O₁₃, with tetrahedrally coordinated carbon, and Fe₁₃O₁₉, synthesized at deep mantle
233 conditions. *American Mineralogist*, 100 2001-2004.
- 234 Merlini, M., Sapelli, F., Fumagalli, P., Gatta, G.D., Lotti, P., Tumiati, S., Abdellatief, M., Lausi, A., Plaisier, J.,
235 Hanfland, M., Crichton, W., Chantel, J., Guignard, J., Meneghini, C., Pavese, A., and Poli, S. (2016)
236 High-temperature and high-pressure behavior of carbonates in the ternary diagram CaCO₃-MgCO₃-
237 FeCO₃. *American Mineralogist*, 101, 1423–1430.
- 238 Merrill, L., and Bassett, W.A. (1975) The crystal structure of CaCO₃(II), a high-pressure metastable phase of
239 calcium carbonate. *Acta Crystallographica*, B31, 343–349.
- 240 Oganov, A.R., Glass, C.W., and Ono, S. (2006) High-pressure phases of CaCO₃: crystal structure prediction
241 and experiment. *Earth and Planetary Science Letters*, 241, 95–103.
- 242 Oganov, A.R., Hemley, R.J., Hazen, R.M., and Jones, A.P. (2013) Structure, bonding, and mineralogy of
243 carbon at extreme conditions. *Reviews in Mineralogy and Geochemistry*, 75, 47–77.
- 244 Oganov, A.R., Ono, S., Ma, Y.M., Glass, C.W., and Garcia, A. (2008) Novel high-pressure structures of
245 MgCO₃, CaCO₃ and CO₂ and their role in Earth's lower mantle. *Earth and Planetary Science Letters*,
246 273, 38–47.
- 247 Oszlányi, G., and Suto, A. (2010) Ab initio structure solution by charge flipping. *Acta Crystallographica*, A60,
248 134–141.
- 249 Oxford Diffraction (2008) CrysAlis RED, ver. 1.171.32.29. Oxford Diffraction, U.K.
- 250 Palatinus, L., and Chapuis, G. (2007) SUPERFLIP—a computer program for the solution of crystal structures
251 by charge flipping in arbitrary dimensions. *Journal of Applied Crystallography*, 40, 786–790.
- 252 Petříček, V., Dušek, M., and Palatinus, L. (2014) Crystallographic Computing System JANA2006: General
253 features. *Zeitschrift für Kristallographie-Crystalline Materials*, 229, 345–352.
- 254 Pickard, C. J., and Needs, R. J. (2015). Structures and stability of calcium and magnesium carbonates at
255 mantle pressures. *Physical Review B*, 91(10), 104101.
- 256 Smith, E.M., Shirey, S.B., Nestola, F., Bullock, E.S., Wang, J.H., Richardson, S.H., Wang, W.Y. (2016) Large
257 gem diamonds from metallic liquid in Earth's deep mantle. *Science*, 354, 1403-1405.
- 258
- 259

260 **Acknowledgments**

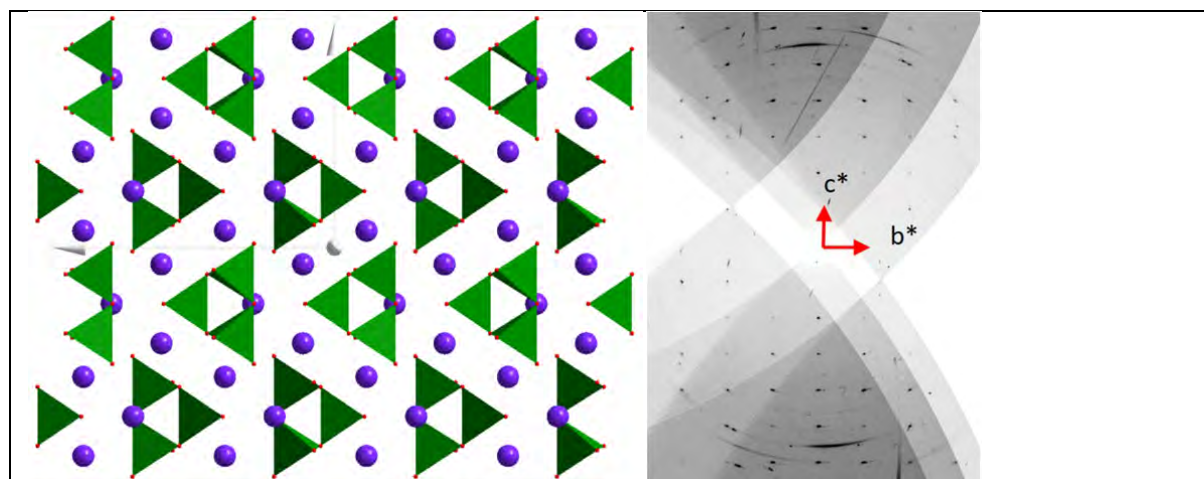
261 We acknowledge ESRF for provision of beamtime (experiments HS-4720 and ES-142). Andrea Risplendente
262 is acknowledged for microprobe analysis in Milan. We acknowledge the Deep Carbon Observatory (DCO)
263 for supporting the research.



264

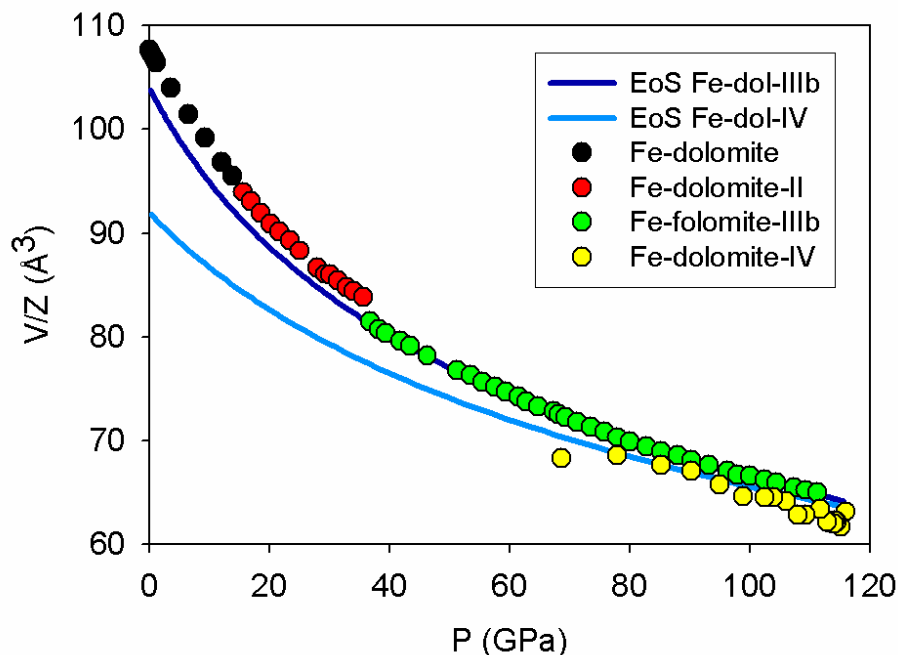
265 Figure 1 – structure of Fe-dolomite-IIIb viewed down [001] and down [010], and reconstruction of
266 reciprocal plane a^*b^* using experimental X-ray data collected at 60 GPa.

267



268 Figure 2 – Crystal structure of dolomite IV and projection of b^*c^* reciprocal space layers from experimental
269 X-ray data collected at 115 GPa after high temperature annealing.

270



271

272 Figure 3 – Experimental volume data (normalized per formula units, V/Z) for Fe-dolomite polymorphs. The
 273 2nd order EoS for Fe-dolomite IIIb and IV polymorphs are also plotted

274

P (GPa)	Annealing T (K)	Phase	Unit cell a, b, c (Å), α, β, γ (°), V (Å ³)	Space Group	Formula, Z	2 nd order BM-EoS: K_0 (GPa), V_0/Z (Å ³)
0.001	298	Fe-dolomite	4.8165(2), 4.8165(2), 16.079(1), 90, 90, 120, 323.0(3)	$R-3$	$\text{Ca}(\text{Mg}_{0.6}\text{Fe}_{0.4})(\text{CO}_3)_2$ $Z=3$	91.7(10), 107.7(3)
15.58	298	Fe-dolomite-II	4.7293(19), 5.6217(15), 7.282(3), 103.84(3), 89.74(3), 91.62(3), 187.90(1)	$P-1$	$\text{Ca}(\text{Mg}_{0.6}\text{Fe}_{0.4})(\text{CO}_3)_2$ $Z=2$	83(3), 108.1(3)
36.81	298	Fe-dolomite-IIIb	12.010(3), 12.010(3), 13.700(5), 90, 90, 120, 1711.34(5)	$R3$	$\text{Ca}(\text{Mg}_{0.6}\text{Fe}_{0.4})(\text{CO}_3)_2$ $Z=21$	91(9), 104(1)
115.18	2500	Fe-dolomite-IV	10.091(3), 8.090(7), 4.533(3), 90, 90, 90, 370.1(4)	$Pnma$	$\text{Ca}(\text{Mg}_{0.6}\text{Fe}_{0.4})(\text{CO}_3)_2$ $Z=6$	150(25), 92(1)
0.001	298	Dolomite	4.8078(2), 4.8078(2), 16.008(1), 90, 90, 120, 320.4(3)	$R-3$	$\text{CaMg}(\text{CO}_3)_2$ $Z=3$	95(1), 106.9(3)
18.16	298	Dolomite-II	4.714(3), 5.574(2), 7.232(4), 103.57(4), 89.49(5), 91.62(4), 184.6(2)	$P-1$	$\text{CaMg}(\text{CO}_3)_2$ $Z=2$	76(3), 110(1)
41.5	298	Dolomite-IIIc	4.455(3), 11.239(6), 13.714(11), 111.13(6), 91.29(6), 89.77(5), 640.3(8)	Possibly $P1$	$\text{CaMg}(\text{CO}_3)_2$ $Z=8$	92(6), 105(1)

275

276 Table 1 – lattice parameters, structural and elastic data for the different polymorphs of Fe-dolomite and
 277 dolomite.

278

279

280